RESEARCH ARTICLE

Design of Power Density Improvement by Applying Novel Shape of Slit and Notch to Outer Rib of Rotor of Spoke-type Permanent Magnet Synchronous Motor

Hyungkwan Jang, Sooyoung Cho, Kang Seok Lee, Ye Jun Oh and Ju Lee[*]

Department of Electrical Engineering, Hanyang University, P.O. Box: 04763, Seoul, South Korea

Abstract:

Objective:

In this study, improvement of power density by applying novel shape of slit and notch to outer ribs of a rotor that reduces magnetic flux leakage in outer rib and increases air-gap magnetic flux density for spe PMSM for a washing machine, was investigated.

Methods:

It is important that motors for home appliance require lower manufacturing cost, high power and high efficiency. In order to increase power, rotor shape is re-designed. In the outer rib of the rotor, magnetic flux leakage occurs by permanent magnet and magnetic flux is saturated which is one of the factors that reduces the power and efficiency. However, if the outer rib is designed to be too thin, the permanent magnet may scatter during high-speed rotation. Therefore, a design considering permanent magnet scattering is necessary. Motor for a washing machine has two operating points that washing mode at constant torque point and dehydrating mode at high-speed point.

Conclusion:

For improvement of higher power density, 2-D finite elements analysis was performed to optimize the parameters of the shape of slit and notch to increase the torque. The torque increases by optimizing width and length of slit shape and notch shape. Finally, with the optimized parameters of shape of slit and notch, stack length was adjusted as per torque requirement for a washing machine motor and power density increases considering the safe factor from stiffness analysis.

Keywords: Spoke-type PMSM, Ferrite permanent magnet, Magnetic flux leakage, Power density, High efficiency, Rotor shape, Stack length.

1. INTRODUCTION

As energy efficiency becomes more important, the use of permanent magnet synchronous motor (PMSM) for home appliances is more increased than conventional induction motors. Induction motors are used widely because of having advantages of low cost and good robustness. However, it has lower efficiency than PMSM [1]. In the recent years, a ferrite permanent PMSM having a high power density has been widely used for home appliance washing machine motors. The washing machine motor has different driving torques and speeds in the washing mode and the dehydrating mode. Therefore, a motor that satisfies both the required torque in the washing mode and dehydrating mode should be designed [2]. A PMSM is divided into SPMSM and IPMSM categories. For the SPMSM, only magnetic torque is generated by permanent magnets. However, the IPMSM use magnetic torque by permanent magnet and reluctance torque by inductance difference of *d*-axis and *q*-axis [3, 4]. IPMSM is used in many industry fields due to the high

[*] Address correspondence to this author at the Department of Electrical Engineering, Hanyang University, P.O. Box: 04763, Seoul, South Korea; Tel: +82-2-2220-0342; E-mail: julee@hanyang.ac.kr

efficiency and power density [5 - 8]. The spoke-type PMSM has a structure in which permanent magnets are inserted into the rotor, and are classified into the IPMSM category [9]. Also, it has advantages of using both magnetic torque and reluctance torque. In addition, as the spoke-type PMSM has a magnetic flux concentrating structure, it can improve the power and replace the rare-earth permanent magnets with relatively inexpensive ferrite permanent magnet [10]. From industrial point of view, the methods of reducing the volume of the motor in order to lower the manufacturing cost are actively studied [11 - 14]. Even though, the power of ferrite PMSM is lower than the power of rare-earth permanent magnet because of its lower magnetic density, there is no eddy current loss on permanent magnet due to the characteristic of ferrite material, which means to minimize the total loss. The spoke-type PMSM has high harmonics and distortion of air-gap magnetic flux density because the magnetic flux are concentrated to direction of rotating, which generates the back-electromotive force (back-EMF), cogging torque and torque ripple [15, 16].

To increase power, it is necessary to modify the shape of the rotor. It can be expected that magnetic flux density transmitting to the air gap can increase by reducing magnetic flux leakage in the ribs. When magnetic flux density transmitting to the air gap should increase [17], power will increase. Furthermore, there is a method to increase the torque by extending stack length. However, in case of the spoke-type PMSM, there is a case where the torque is not improved with the increase in the axial length due to the axial magnetic flux leakage [12].

In this study, the shape of the rotor of the spoke-type PMSM for a washing machine was redesigned to improve the power density by reducing leakage flux using 2-D finite element analysis (FEA). In the section 2, output characteristics and design parameters of basic motor for a washing machine were analyzed. In section 3, the width and length of the slit shape and notch shape were optimized to improve the torque and then satisfy the safe factor during high-speed rotation by stiffness analysis. Finally, the power density increases by reducing the stack length in the final model to meet the required output condition of the washing machine motor.

2. ANALYSIS OF THE SPOKE-TYPE PMSM FOR THE WASHING MACHINE

2.1. Design Conditions and Parameters

Table **1** shows the design condition of the basic model of the spoke-type PMSM for the washing machine. The diameter of rotor is 60% of the diameter of the stator. The coil is 0.8 mm diameter of aluminum and teeth concentrated winding was applied with a fill factor of 0.45.

Table 1. Design condition of the basic model for washing machine.

Design condition	Value	Design condition	Value
Diameter of stator [mm]	83	Stacking length [mm]	46
Diameter of rotor [mm]	50	Rated phase current [A_{rms}]	2.2
Pole/Slot	8/12	Current density [$A_{rms/mm}^{2}$]	4.3
Ratio of gear	11.6:1	DC-Link voltage [V]	310

2.2. Analysis of Required Output Condition and Characteristic of the Basic Model

The washing machine has a gear with a ratio of 11.6:1, as shown in Table **1**, connected to the spoke-type PMSM. Table **2** shows the required output condition of the spoke-type PMSM for the washing machine.

Table 2. Required output of the spoke-type PMSM.

-	Value	
	Washing mode	**Dehydrating mode**
Torque [Nm]	1.12	0.80
Speed [rpm]	3480	8584
Efficiency [%]	90.8	93.7
Power [W]	408	731
Power density [W/kg]	326.66	585.26

On the washing mode, a pulsator of the washing machine rotates at 300 rpm when the spoke-type PMSM rotates at 3480 rpm. For dehydrating mode, a washing machine tub rotates at 740 rpm when the spoke-type PMSM rotates at 8584 rpm. The required torque should be 1.12 Nm for washing mode and 0.80 Nm for dehydrating mode. The back-

EMF should not exceed the voltage limit of 161 V by the DC link according to Table **1**. Fig. (**1**) shows the torque-speed curve of the constant power characteristic of the basic model.
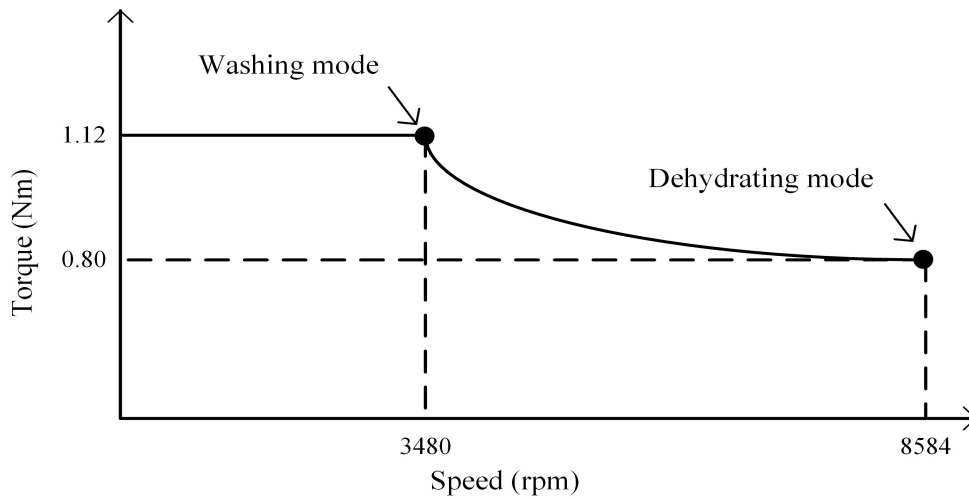

Fig. (1). Torque and speed curve of spoke-type PMSM for a washing machine.

In this paper, the stator shape is not modified and the rotor shape is re-designed to reduce the manufacturing cost and improve the power density. Fig. (**2a**) presents the basic model and Fig. (**2b**) shows the distribution of magnetic flux density at 3480 rpm. It is well known factor that magnetic flux leakage decreasing the power and the efficiency occurred and saturated on the inner rib and outer rib in shown the Fig. (**2b**). Hence, this is a method of improving the torque by reducing the magnetic flux leakage, while satisfying the rotor stiffness at high-speed.
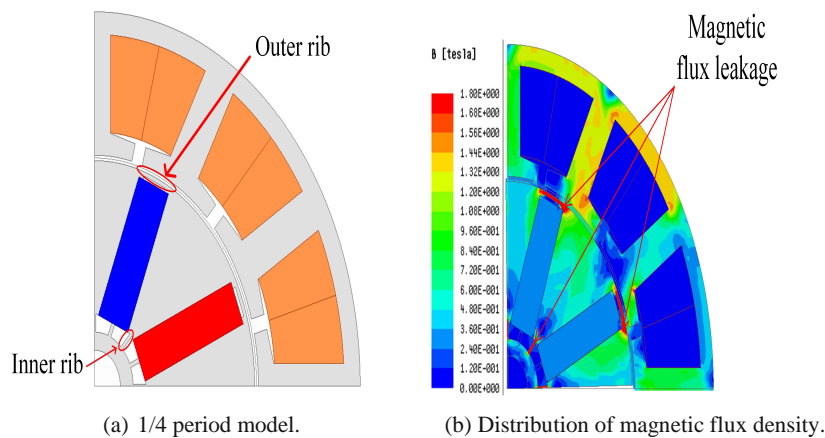

(a) 1/4 period model.   (b) Distribution of magnetic flux density.

Fig. (2). Basic model of the spoke-type PMSM for a washing machine.

3. RE-DESIGN OF ROTOR WITH SLIT SHAPE AND NOTCH SHAPE FOR IMPROVEMENT OF POWER DENSITY

3.1. A Method of Applying the Shape of Slit and Notch

Fig. (**3**) shows the parameters of slit shape and notch shape. Parts of re-design are divided into two parts, one is slit shape and another one is notch shape. First, making the groove with the slit shape applied to the outer rib. Second, making the groove of the notch shape at both ends of the permanent magnet with thickness of 5 mm.

In case of slit shape grooves, ① and ② are the width and length of the slit shape applied to the outer rib portion, respectively. The slit shape width is in the radial direction from the end of the rotor to the center of the rotor. In addition, the slit shape length is on both sides with respect to the center of the permanent magnet. The next step is to make the groove of the notch.
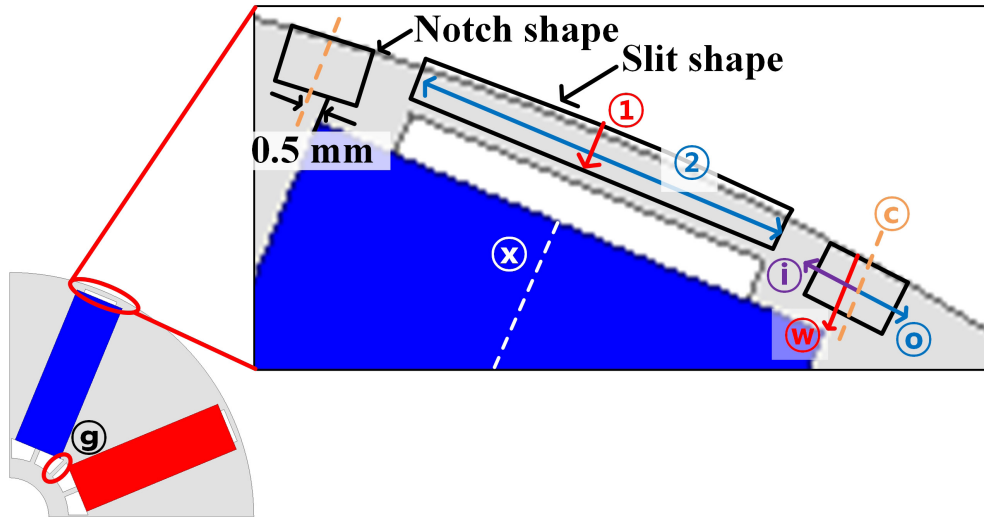
Fig. (3). Design variables of the slit shape and the notch shape.

Shape, so that ⓒ is the center of the notch shape and 0.5 mm away from the end of the permanent magnet. ⓘ and ⓞ denote inner length and outer length of the notch shape, respectively, centered on the center of notch shape. ⓦ represents the notch shape width from the end of the rotor to the center of the rotor in the radial direction. ⓖ indicates the inner rib, which is also the area where magnetic flux leakage and magnetic flux density saturation occur.

In order to increase torque, the inner rib of the rotor was partially removed. This is because the torque increases by removing the inner rib, which affects magnetic flux leakage [18]. The re-design of the rotor flowchart is shown in Fig. (4).
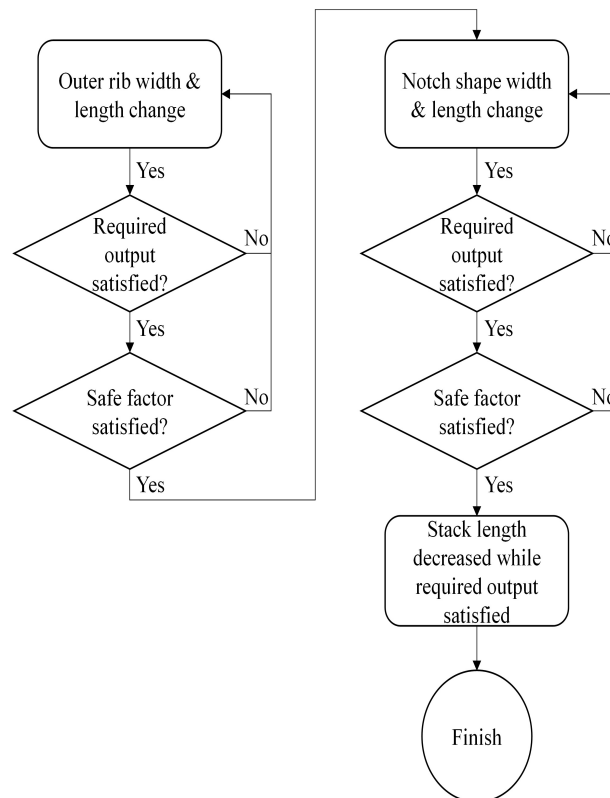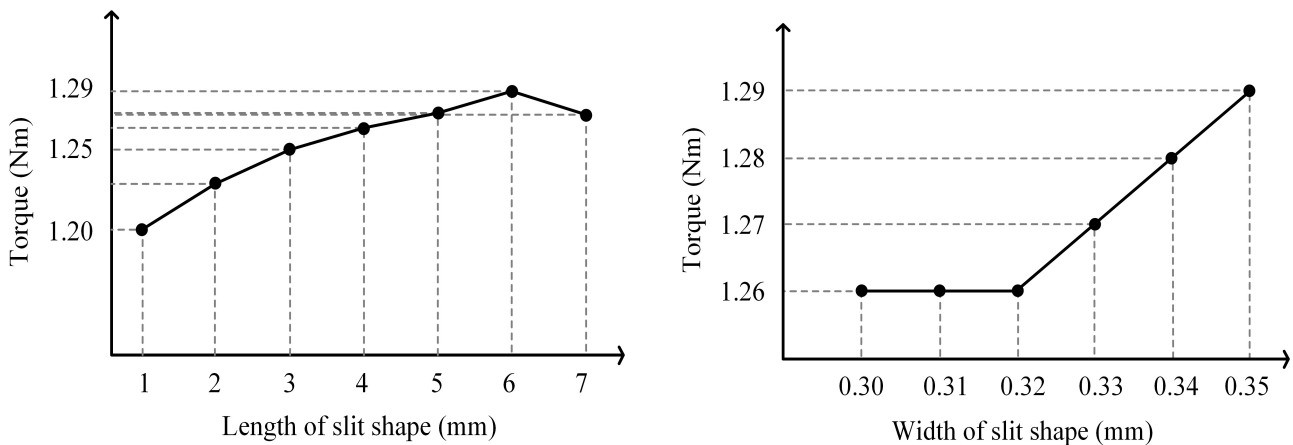

Fig. (4). Flow chart of optimizing shape of slit and notch.

First, we optimize the width and length of the slit shape to improve the torque under the condition that the safe factor is 1.3 or more. Second, the width, inner length, and outer length of the notch shape were optimized when both the safe factor and the torque improvement are satisfied in the same design. In order to improve the power density with the optimized shape of slit and notch, stack length is reduced to meet the required torque and output condition of the spoke-type PMSM for a washing machine. The formula for the safe factor of the motor is expressed in Eq. (1). The ultimate stress of the electric steel sheet used for the washing machine motor is 467 MPa.

$$Safe \ Factor = \frac{Ultimate \ Stress}{Actual \ Stress} \qquad (1)$$

3.2. Re-Design of the Rotor with Slit Shape and Analysis of the Torque

In order to optimize the slit shape applied to the outer rib portion, optimization was performed for the width of the slit shape at first. For reference, the outer rib width of the base model is 0.5 mm. As stated forehead, the width of the slit shape has the direction that enters the center of the rotor in the radial direction from the end of the rotor. Simulation test was carried out and the torque was obtained by changing the slit shape width from 0 mm to 0.35 mm. In this case, the slit shape length is fixed at 4 mm. Fig. (**5a**) shows that the torque at 3480 rpm increases as the slit shape width increases.

(a) Torque at 3480 rpm by various slit shape width.

(b) Torque at 3480 rpm by various slit shape length.

Fig. (5). Torque at 3480rpm by various width and length of slit shape.

It can be seen that a tendency that the air-gap magnetic flux density transmitted to the air gap increases as the leakage magnetic flux decreases. Fig. (**5b**) shows the torque according to the change of the slit shape length with the slit shape width of 0.33 mm optimized in previous step. As the slit shape length increases, the torque increases, but at 7 mm, the torque tends to decrease. The reason is that when the slit shape length is 7 mm, magnetic resistance increases that affect of the magnetic flux transmitted to the air-gap. Therefore, when the slit shape length is 6 mm, the maximum torque can be determined to be 1.29 Nm at 3480 rpm. In Fig. (**6**), the torque on dehydrating mode is 0.80 Nm @ 8584 rpm and the back-EMF is 161.0V, satisfying both the required output conditions.

In the stiffness analysis, maximum stress occurs around the corner of ribs when a rotor is rotating at high speed. Thickness of the ribs should be appropriate thickness that the permanent magnet is prevented from scattering. Considering the safe factor, the actual stress is 391.1 MPa is shown in Table **3** when the slit shape width is 0.34 mm. It means that the safe factor is 1.19, which cannot meet the required safe factor of 1.3. On the another hand, the slit shape width of 0.33 mm meets the required safe factor and the torque is 1.27 Nm at 3480 rpm. For the result of stiffness analysis with the optimized slit shape, the actual stress is 313.36 MPa at 8584 rpm as shown in Fig. (**7**) and the safe factor is 1.49.
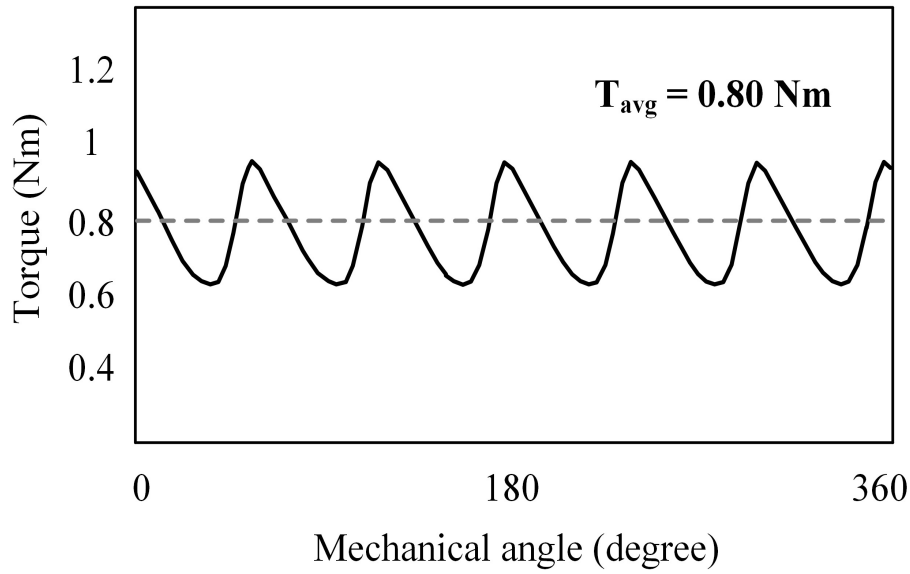
Fig. (6). Torque at 8584 rpm with optimized slit shape.

Table 3. Result of stiffness analysis by 0.33 mm and 0.34 mm of slit shape width.

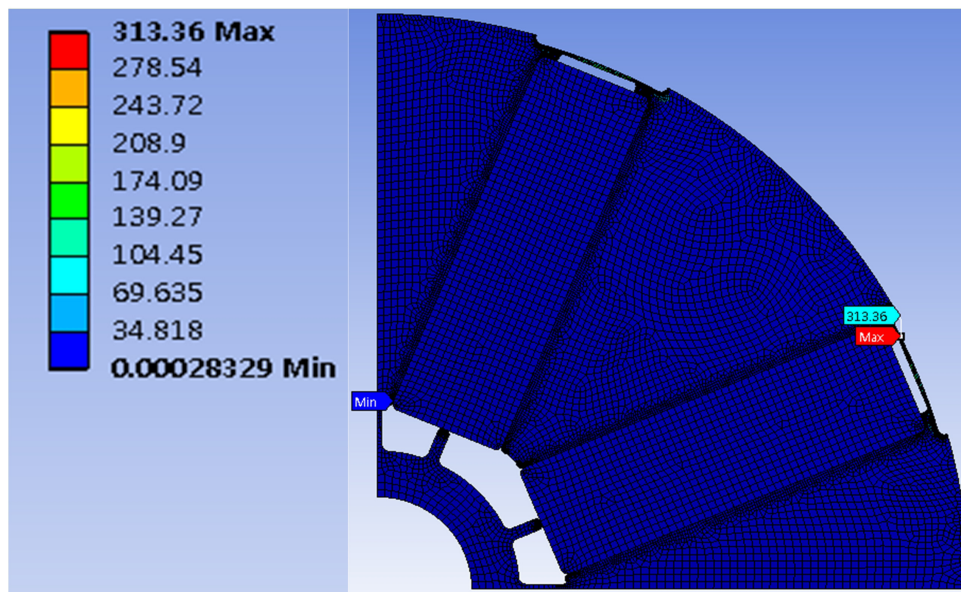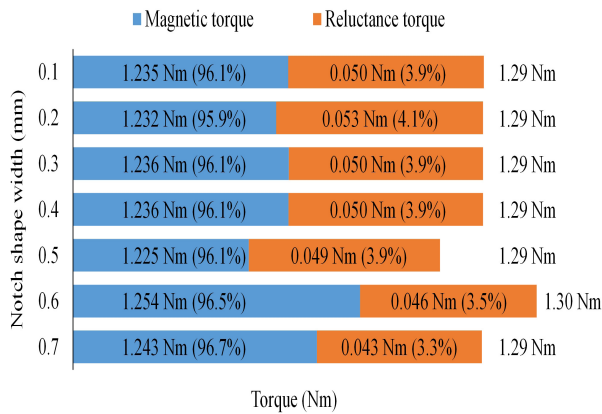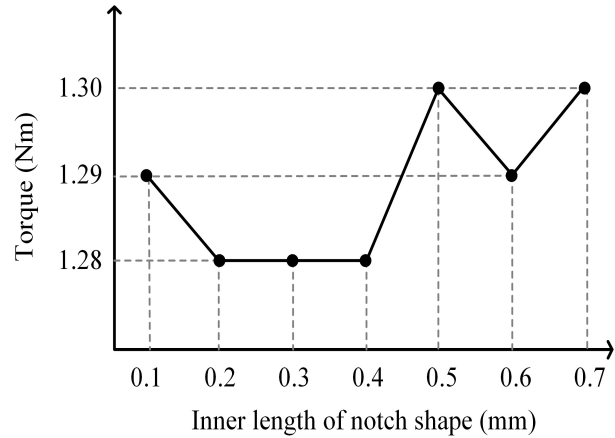|	0.33 mm of slit shape width	0.34 mm of slit shape width
Actual Stress [MPa]	313.36	391.10
Safe factor	1.49	1.19

Fig. (7). Result of stiffness analysis at 8584 rpm with the optimized slit shape.

3.3. Re-Design of the Rotor with Notch Shape and Analysis of the Torque

In the 3.2 session, we optimized the width and length of the slit shape and the torque improved by 15.2% compared to the base model. As a final shape, additional torque enhancement was carried out by adding a notch shape to the optimized slit shape. The inner length of notch shape was fixed at 1 mm to optimize the width of notch shape. Fig. (**8a**) shows the torque along the changes of the notch shape width.

(a) Torque at 3480 rpm by various notch shape width.

(b) Torque at 3480 rpm by various notch shape inner length.

Fig. (8). Torque at 3480 rpm by various width and inner length of notch shape.

A constant torque of 1.29 Nm at 3480 rpm was obtained with the notch shape width of 0.1 mm to 0.5 mm. However, when the notch shape width is 0.6 mm, the torque increases to 1.30 Nm at 3480 rpm and saturates. The reason for the increase in torque at the notch shape width of 0.6 mm is that the area of the outer rib related to the *q*-axis inductance decreases as shown in Table **4**. When the notch shape width is 0.6 mm, the inductance difference is found to be between the *d*-axis and *q*-axis, which generates the reluctance torque, and the reluctance torque decreases according to Eq. (2). In contrast to the reluctance torque phenomenon, the magnetic torque is analyzed to be relatively larger than the reluctance torque as the air gap magnetic flux linkage increases.

Table 4. Inductance changes by notch shape width.

Notch shape width [mm]	0.1	0.2	0.3	0.4	0.5	0.6	0.7
Inductance of *d-axis* [H]	13.55	13.23	13.57	13.56	13.49	13.54	13.57
Inductance of *q-axis* [H]	17.06	16.95	17.06	17.06	16.96	16.70	16.57
L_d-L_q [H]	-3.51	-3.73	-3.49	-3.50	-3.47	-3.16	-3.00

$$T = \frac{3}{2}\frac{P}{2}[\psi_a i_q + (L_d - L_q)i_d i_q] \tag{2}$$

Where P is the number of magnetic poles, ψ_a is the linkage flux by the permanent magnets, i_d is the current of *d*-axis, i_q is the current of *q*-axis, L_d is the inductance of *d*-axis, and L_q is the inductance of *q*-axis.

Therefore, the notch shape width of 0.6 mm is the optimal value, and torque is analyzed through various outer lengths of the notch shape in the next step. In Section 3.2, when the slit shape length is 7 mm or more, the magnetic resistance is increased affecting the flow of magnetic flux transmitted to the air-gap and the torque decreased. In a similar trend, when the outer length of the notch shape is simulated from 0 mm to 0.5 mm, the change in torque is not apparent, so the notch shape outer length of 0 mm is determined. For the next step, Fig. (**8b**) shows the result of optimizing the inner length of the notch shape with the optimized width and outer length of the notch shape. When the inner length of the notch shape is 0.5 mm, the torque is 1.30 Nm at 3480 rpm and saturated. The torque on the dehydrating mode is 0.80 Nm at 8584 rpm and the back-EMF is satisfied as 160.7 V.

Fig. (**9**) shows the final model with the optimized slit and notch shape. Comparision of torque between the basic and final model is shown in Fig. (**10**). The torque improved 16% from 1.12 Nm to 1.30 Nm. The result of stiffness analysis at 8584 rpm, the dehydrating mode of the final model is shown in Fig. (**11**). As a result of the stiffness analysis of the final model, the actual stress is 330.83 MPa and the safety factor is 1.4, satisfying the requirement of 1.3.
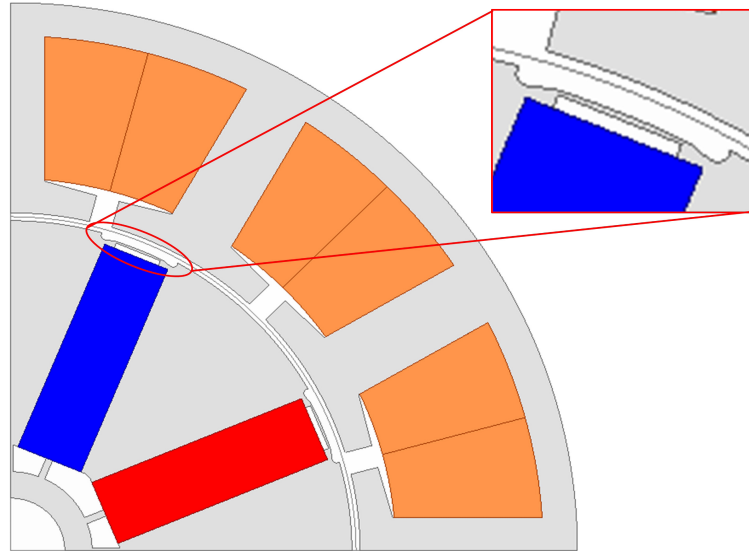
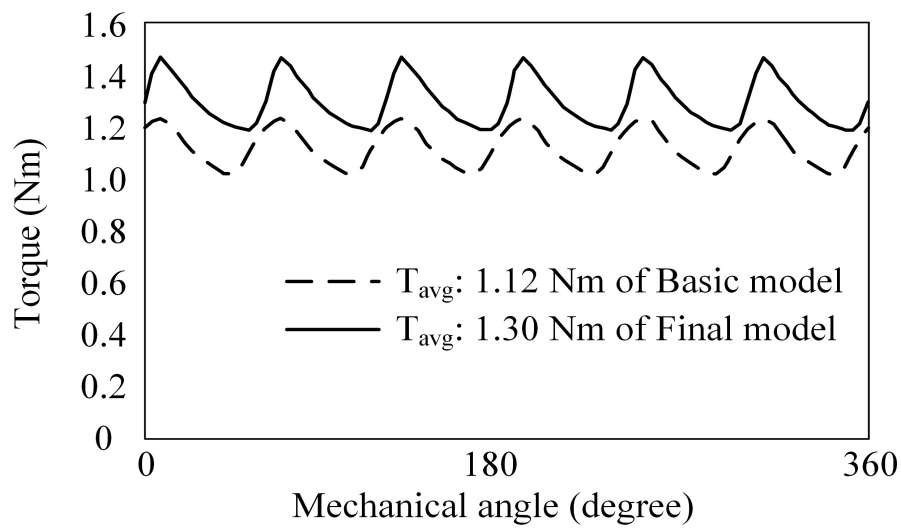**Fig. (9).** Final optimized model of spoke-type PMSM for a washing machine.

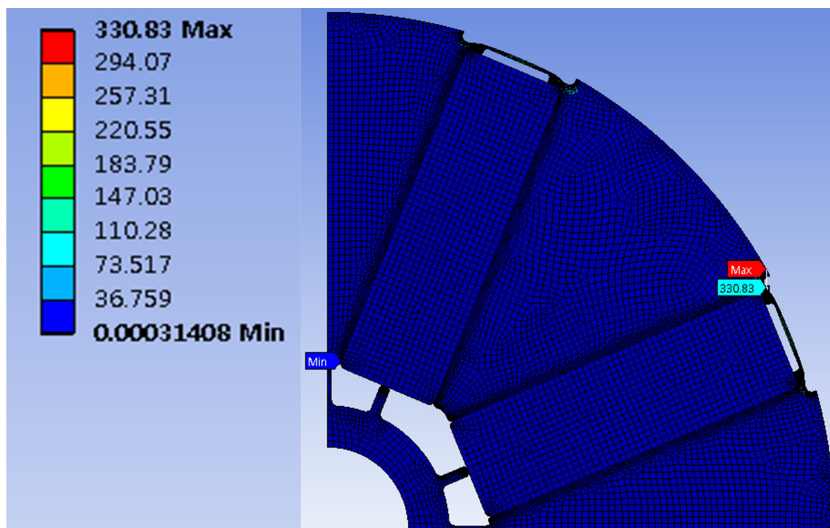**Fig. (10).** Torque of final model compared with the basic model.

Fig. (11). Result of stiffness analysis of the final model.

3.4. Decreasing Stack Length for the Requirement of the Spoke-Type PMSM for a Washing Machine

In Sections 3.2 and 3.3, the shape of slit and notch were optimized and the torque increases to 1.30 Nm at 3480 rpm, which is increased to16% as compared to the basic model. In order to enhance the power density, it is necessary to reduce the stack length of the final model to meet the output requirements of the motor for a washing machine. Reducing the stack length can improve the power density and save manufacturing costs. The required torque of the washing machine motor is 1.12 Nm at 3480 rpm and 0.80 Nm at 8584 rpm, as shown in Table **2**. Fig. (**12**) represents the torque analysis by varying the stack length to obtain the the required torque.
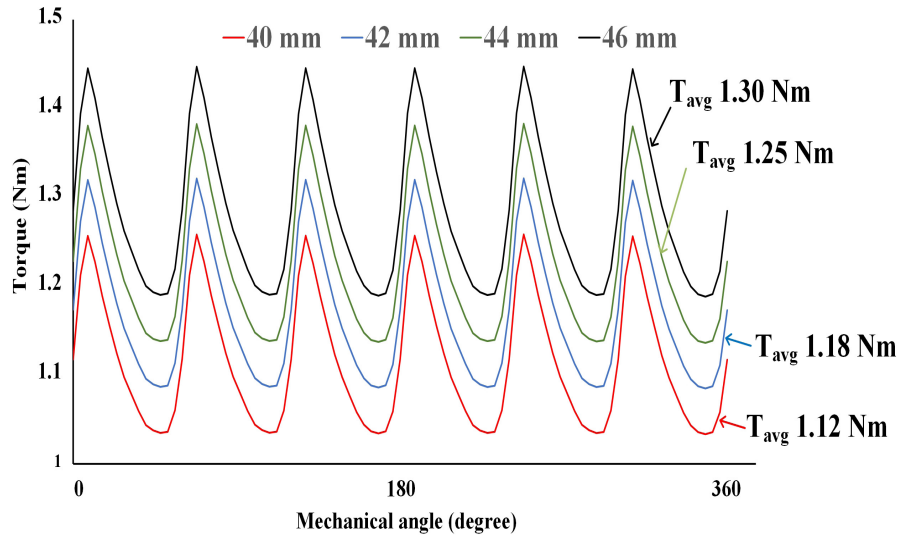

Fig. (12). Torque of Final model at 3480 rpm by various stack length.

The spoke-type PMSM generates the magnetic torque and the reluctance torque. When the stack length reduces, the torque decreases linearly as follows [19];

$$T \quad \frac{}{4} k_w B_{g1} ac \cos \quad D_g^2 L_{stk} \quad \frac{1}{16} \frac{1}{p} k_w^2 ac^2 G_{a1} \sin 2 \quad D_g^3 L_{stk} \tag{3}$$

Where K_w is the winding factor, B_{g1} is the fundamental wave magnitude of air-gap magnetic flux density, *ac* is the electric loading, D_g is the diameter of air gap, L_{stk} is the stack length, G_{a1} is fundamental wave magnitude of relative air-gap permeance.

The final stack length satisfying the required output of the spoke-type PMSM for a washing machine is 40 mm, which is 6 mm smaller than the basic model. The output characteristics of the basic model and the final model is shown in Table **5**. The power density of the final model on the washing mode was improved by 15% and the efficiency by 0.7% compared with the basic model. The power density on the dehydration mode was improved by 14.5% and the efficiency was improved by 0.2%.

Table 5. Comparing output characteristic with the basic model and the final model.

-	Basic model		Final model	
	Washing mode (3480rpm)	**Dehydrating mode (8584 rpm)**	**Washing mode (3480rpm)**	**Dehydrating mode (8584 rpm)**
Stack length [mm]	46	46	40	40
Torque [Nm]	1.12	0.80	1.12	0.81
Power density [W/kg]	326.66	585.26	375.72	670.38
Efficiency [%]	90.8	93.7	91.5	93.9
Phase back-EMF [V_{peak}]	106.4	160.7	98.9	160.7

CONCLUSION

In this study, 2-D finite elements analysis was performed to reduce magnetic flux leakage and to improve the torque by applying the novel shape of the slit and notch to outer rib portion of the rotor. With the optimized slit shape and notch shape, the stack length reduces for the requirement of the output characteristic for a washing machine motor and the power density improved. The redesigned rotor shape improved the torque by 16% by applying a slit shape and notch shape to the outer rib portion. In addition, the power density is improved by 15% by optimizing the stack length to match the required output of the washing machine motor.

For further research, the novel rotor shape obtained through this study would be actually manufactured and the output will be verified by performing actual tests.

CONSENT FOR PUBLICATION

Not applicable.

CONFLICT OF INTEREST

ACKNOWLEDGEMENTS

REFERENCES

[1]   W. Zhao, T.A. Lipo, and B. Kwon, "Torque pulsation minimization in spoke-type interior permanent magnet motors with skewing and sinusoidal permanent magnet configurations", *IEEE Trans. Magn.,* vol. 51, no. 11, p. 8110804, 2015.
[http://dx.doi.org/10.1109/TMAG.2015.2442977]

[2]   K.Y. Hwang, J.H. Jo, and B.I. Kwon, "A study on optimal pole design of spoke-type IPMSM with concentrated winding for reducing the torque ripple by experiment design method", *IEEE Trans. Magn.,* vol. 45, no. 10, pp. 4712-4715, 2009.
[http://dx.doi.org/10.1109/TMAG.2009.2022645]

[3]   H. Tachibana, M. Sanada, S. Morimoto, and Y. Inoue, "Study on the ratio of outer diameter to stack length suitable for high torque and high power in IPMSMs", *2012 15th International Conference on Electrical Machines and Systems (ICEMS),* Sapporo, Japan, 2012.

[4]   S. Cho, H. Ahn, H.C. Liu, H. Hong, J. Lee, and S. Go, "Analysis of inductance according to the applied current in spoke-type PMSM and suggestion of driving mode", *IEEE Trans. Magn.,* vol. 53, no. 6, p. 8202404, 2017.
[http://dx.doi.org/10.1109/TMAG.2017.2662719]

[5]   P. Liang, F. Chai, Y. Li, and Y. Pei, "Analytical prediction of magnetic field distribution in spoke-type permanent-magnet synchronous machines accounting for bridge saturation and magnet shape", *IEEE Trans. Ind. Electron,* vol. 64, no. 5, pp. 3479-3488, May. 2017.

[6]   W. Fei, B. Xia, and J. Shen, "Design of spoke-type ferrite interior permanent magnet synchronous machines considering the number of rotor poles", *2017 20th International Conference on Electrical Machines and Systems (ICEMS),* 2017 Sydney, NSW, Australia

[7]   H. Jun, J. Lee, G. Yoon, and J. Lee, "Optimal design of the PMSM retaining plate with 3-D barrier structure and eddy-current loss-reduction effect", *IEEE Trans. Ind. Electron.,* vol. 65, no. 2, pp. 1808-1818, 2018.
[http://dx.doi.org/10.1109/TIE.2017.2736501]

[8]   R.T. Ugale, and B.N. Chaudhari, "Rotor configurations for improved starting and synchronous performance of line start permanent-magnet synchronous motor", *IEEE Trans. Ind. Electron.,* vol. 64, no. 1, pp. 138-148, 2017.
[http://dx.doi.org/10.1109/TIE.2016.2606587]

[9]   R.N. Firdaus, R. Suhairi, S. Farina, K.A. Karim, and Z. Ibrahim, "Improvement of power density spoke type permanent magnet generator", *2015 IEEE 11th International Conference on Power Electronics and Drive Systems,* 2015 Sydney, NSW, Australia

[10]   M. Kimiabeigi, J.D. Widmer, R. Long, Y. Gao, J. Goss, R. Martin, T. Lisle, J.M. Vizan, A. Michaelides, and B.C. Mecrow, "On selection of rotor support material for a ferrite magnet spoke-type traction motor", *IEEE Trans. Ind. Appl.,* vol. 52, no. 3, pp. 2224-2233, 2016.
[http://dx.doi.org/10.1109/TIA.2016.2530722]

[11]   H. Seol, T. Jeong, H. Jun, J. Lee, and D. Kang, "Design of 3-times magnetizer and rotor of spoke-type PMSM considering post-assembly magnetization", *IEEE Trans. Magn.,* vol. 53, no. 11, p. 8208005, 2017.
[http://dx.doi.org/10.1109/TMAG.2017.2707593]

[12]   S. Lee, J. Lee, and W. Kim, "A study on correcting the nonlinearity between stack length and back electromotive force in spoke type ferrite magnet motors", *IEEE Trans. Magn.,* vol. 53, no. 6, p. 8201404, 2017.

[http://dx.doi.org/10.1109/TMAG.2017.2655059]

[13]   M.M. Rahman, K. Kim, and J. Hur, "Design and optimization of neodymium-free spoke-type motor with segmented wing-shaped PM", *IEEE Trans. Magn.,* vol. 50, no. 2, p. 7021404, 2014.
[http://dx.doi.org/10.1109/TMAG.2013.2282151]

[14]   A. Tap, L. Xheladini, T. Asan, M. Imeryuz, M. Yilmaz, and L.T. Ergene, "Effects of the rotor design parameters on the torque production of a PMaSynRM for washing machine applications", *2017 International Conference on Optimization of Electrical and Electronic Equipment (OPTIM) & 2017 Intl Aegean Conference on Electrical Machines and Power Electronics (ACEMP),* Brasov, Romania, 2017.

[15]   H. Nak, M.O. Gulbahce, M. Gokasan, and A.F. Ergenc, "Performance investigation of extended Kalman filter based observer for PMSM using in washing machine applications", *2015 9th International Conference on Electrical and Electronics Engineering (ELECO),* 2015 Bursa, Turkey

[16]   X. Liu, H. Chen, J. Zhao, and A. Belahcen, "Research on the performances and parameters of interior PMSM used for electric vehicles", *IEEE Trans. Ind. Electron.,* vol. 63, no. 6, pp. 3533-3545, 2016.
[http://dx.doi.org/10.1109/TIE.2016.2524415]

[17]   H. Kim, and J. Moon, "Improved rotor structures for increasing flux per pole of permanent magnet synchronous motor", *IET Electr. Power Appl.,* vol. 12, no. 3, pp. 415-422, 2017.
[http://dx.doi.org/10.1049/iet-epa.2017.0432]

[18]   X. Ge, Z.Q. Zhu, J. Li, and J. Chen, "A spoke-type IPM machine with novel alternate airspace barriers and reduction of unipolar leakage flux by step-staggered rotor", *IEEE Trans. Ind. Appl.,* vol. 52, no. 6, pp. 4789-4797, 2016.
[http://dx.doi.org/10.1109/TIA.2016.2600649]

[19]   J.N. Bae, " Permanent magnet synchronous machine design through an automatic selection of the specific loadings", *Ph.D. Thesis,* Hanyang University, Seoul, South Korea, 2010.